PAPER

# Physical properties of ordered mesoporous SBA-15 silica as immunological adjuvant*

IOP Publishing Journal of Physics D: Applied Physics
J. Phys. D: Appl. Phys. **47** (2014) 425402 (10pp) doi:10.1088/0022-3727/47/42/425402

# Physical properties of ordered mesoporous SBA-15 silica as immunological adjuvant*

**F Mariano-Neto[1], J R Matos[3], L C Cides da Silva[3], L V Carvalho[2], K Scaramuzzi[2], O A Sant'Anna[2], C P Oliveira[1] and M C A Fantini[1]**

[1] Instituto de Física, Universidade de São Paulo, Caixa Postal 66318, 05314-970, São Paulo, SP, Brazil
[2] Instituto Butantan, Av. Vital Brasil 1500, 05503-900, São Paulo, SP, Brazil
[3] Instituto de Química, Universidade de São Paulo, Caixa Postal 26077, 05513-970, São Paulo, SP, Brazil

E-mail: mfantini@if.usp.br

Received 30 May 2014, revised 26 August 2014
Accepted for publication 29 August 2014
Published 24 September 2014

**Abstract**

This work reports a detailed analysis of the ordered mesoporous SBA-15 silica synthesis procedure that provides a matrix with mean pore diameter around 10 nm. The encapsulation of bovine serum albumin (BSA) by four different methods allowed the determination of the best imbibition condition, which is keeping the mixture under rest and solvent evaporation. Simulation of the *in situ* SAXS scattered intensity of the BSA release in potassium buffer solution, gastrointestinal fluids revealed a slow evolution of BSA content, independent of the media. Proton induced x-ray emission results obtained in calcined mouse organs revealed that silica is only present in the spleen after 35 days and is completely eliminated from all mouse organs after 10 weeks. Biological studies showed that Santa Barbara Amorphous-15 is an effective adjuvant when compared to the traditional $Al(OH)_3$, and is non-toxic to mice, rats, dogs and even cells, such as macrophages and dendritic cells. Recent studies showed that the immunological response is improved by enhancing the inflammatory response and the recruitment of immune competent cells to the site of injection as by the oral route and, most importantly, by increasing the number of phagocytes of a particulate antigen by antigen presenting cells.

Keywords: mesoporous silica, adjuvant, immune response, SAXS

## 1. Introduction

The innovation of Mobil company matter (MCM)- type ordered mesoporous materials (OMM) reported in 1992 [1] and the subsequent development of the Santa Barbara Amorphous (SBA)-type of ordered mesoporous silica (OMS) in 1998 [2] made a breakthrough in the area of porous systems. Many applications became possible and were spread in science, ranging from traditional areas such as adsorption and catalysis to environmental use [3], nanotechnology [4] and biotechnology [5–9]. In particular, SBA-15 can act as an antigen delivery system, enhancing antibody responsiveness [10]. More recently, the use of SBA-15 in oral vaccinations was reported [11] and the effect of the silica morphology to enhance mucosal and systemic immune response was also proved [12]. A review paper was published in 2013 reporting the state of art on our pioneer work related to the adjuvant properties of OMS [13]. The aim of the present work is to complement our previous studies [9, 10] on the use of SBA-15 as an immunological vehicle, focusing on the synthesis process and physical properties of SBA-15 OMS in order to control its performance to the uptake of biomolecules. The reproducibility of the synthesis process, particle size distribution and the incorporation of biologically interesting molecules such as bovine serum albumin (BSA) were tested.

Since 2004 we have pointed out the unusual properties of SBA-15 as an antigen delivery system to form efficient immunogenic complexes [14]. Their uses for oral vaccination constitute a real breakthrough in the concept of mass immunization.

## 2. Materials and methods

### 2.1. Samples

The synthesis procedure presented in [15] was used, such that 4 g of the Pluronic P123 ($PEO_{20}PPO_{70}PEO_{20}$) from BASF was

* This research is under the scope of the International Patent WO 07030901, IN248654, ZA2008/02277, KR 1089400, MX297263, JP5091863, CN101287491B.

 

**Table 1.** Interplanar distances $d_{(hkl)}$, a is the lattice parameter from $d_{(hkl)}$, mean lattice parameter $a_{avg}$ and integrated total area under the diffraction peak A.

| Synthesis | $d_{(100)}$ (nm) | $a$ (nm) | $d_{(110)}$ (nm) | $a$ (nm) | $d_{(200)}$ (nm) | $a$ (nm) | $a_{avg}$ (nm) | $A$ (a.u.) |
|---|---|---|---|---|---|---|---|---|
| 1 | 10.9(1) | 12.6(1) | 6.1(1) | 12.3(1) | 5.3(1) | 12.3(1) | 12.4(2) | 13.8(2) |
| 2 | 11.1(1) | 12.8(1) | 6.2(1) | 12.5(1) | 5.4(1) | 12.4(1) | 12.4(2) | 15.8(2) |
| 3 | 11.0(1) | 12.7(1) | 6.2(1) | 12.4(1) | 5.3(1) | 12.3(1) | 12.5(2) | 12.5(2) |
| 4 | 11.1(1) | 12.8(1) | 6.2(1) | 12.5(1) | 5.4(1) | 12.4(1) | 12.6(2) | 11.3(2) |

dissolved in 122 g of 2M HCl solution and kept under magnetic and mechanical stirring for 1 h. 8.6 g of tetraethyl orthosilicate (from Fluka) was added and the solution was continuously stirred for 24 h. After this process the mixture was submitted to a 48 h hydrothermal treatment at 100 °C in an autoclave, washed with de-ionized water and dried at room temperature. The polymer template was then removed through calcination at 540 °C under $N_2$ for 2 h and in air for 4 h. In total, 10 g of SBA-15 was prepared in four processes. The resulting material of each process was characterized and mixed in order to conduct the biological tests.

Four different samples were prepared with SBA-15 plus BSA, following different mixture pathways. These pathways involved a combination of two methods of mixing (rest and magnetic stirring) and two methods of drying (filtering and evaporation in oven). The resulting samples were named according to the following: SF (stirring and filtering), SE (stirring and evaporation), RF (rest and filtering) and RE (rest and evaporation).

The samples with BSA were prepared in 100 ml of phosphate buffer saline (PBS) solution (pH = 7.4), with the addition of 0.390 g of BSA and 1 g of SBA-15. The BSA/SBA-15 mass ratio was determined in our previous tests of immune response [10]. Two solutions were prepared in this way, with one being kept at rest for 48 h and the other kept under magnetic stirring for the same period of time. These solutions were divided in equal parts, with one of the parts being filtered with 0.25 $\mu$m filter paper and the other being set to 45 °C evaporation process in an electric oven. Some samples were covered with the pH-sensitive polymer Eudragit (anionic polymer of methacrylic acid) in a 1 : 1 mass proportion to SBA-15 in aqueous solution (30% Eudragit) in order to test the release of BSA from SBA-15 plus Eudragit in different test solutions which mimetic physiological conditions.

### 2.2. Experimental techniques

Small angle x-ray scattering (SAXS) characterization was performed using a rotating anode copper target ($\lambda$ = 0.154 18 nm), with line-shaped beam, vacuum path and an image plate detecting system. The diffraction pattern was indexed according to the *p6mm* symmetry group [2], corresponding to a hexagonal bidimensional structure of pores in the ordered portions of the sample. The diffraction peaks were isolated from the small angle scattering through the subtraction of a straight line background under the (1 0 0) peak and another for the (1 1 0) and (2 0 0) peaks. Table 1 presents the obtained results related to the reproducibility of the structural properties of the synthesized material.

Additionally to peak intensity analysis, a theoretical model describing the silica structure was used to analyse the evolution of structural parameters of the material during the BSA release in different conditions. A modified version of the model presented in [21] was used. This model employs a factorization of the scattered intensity into contributions from the form factor and the structure factor. Pore size and spatial distribution are assumed to be independent, which allows for this factorization. The scattered intensity is described by

$$I(q) = (\rho_1 - \rho_2)^2 n_d \left\langle F(q)^2 \right\rangle (1 + \beta(q)\,[\langle Z(q)\rangle - 1]\,G(q)) \tag{1}$$

where $F(q)$ is the scattering amplitude or Fourier transform of the pore shape, $n_d$ is the number density of pores, and $Z(q)$ is the structure factor describing their spatial distribution. The angular brackets denote an average with respect to pore size and spatial distribution. The form factor is composed of a longitudinal factor taken as the form factor of a thin rod while the cross-sectional form factor is

$$P_{CS}(q) = \left(\frac{2J_1(qR)}{qR}\right)^2 \tag{2}$$

with a polydispersity described by $\beta(q)$. The structure factor describes a bidimensional hexagonal lattice, which represents the pore structure of SBA-15 silica, with spatial distortions taken into account by $G(q)$. Detailed expressions for all the factors can be found in [21].

Three extra contributions were added to the scattered intensity due to background effects, accounting for scattering from the microporosity of the walls, the scattering from larger objects and the residual carbonaceous material remaining in the sample holder after polymer decomposition.

The final expression for the scattering intensity is given by

$$\begin{aligned} I(q) = {} & \mathrm{Sc}_1 P_{rod}(q) \left\langle F_{CS}(q)^2 \right\rangle (1 + \beta(q)\,[\langle Z(q)\rangle - 1]\,G(q)) \\ & + I(q)_{chain} + \mathrm{SC} q_{-4} I(q) q_{-4} + \mathrm{SC}_{extra} I(q)_{extra}. \end{aligned} \tag{3}$$

This expression takes into account the spatial distribution and morphology of the pores, and from this expression the x-ray scattering curve representing the bidimensional hexagonal pore structure can be evaluated.

The experimental conditions of the measurements lead to a smearing effect in the experimental data, taken into account in the expression

$$I(\langle q\rangle) = \int R(\langle q\rangle, q)\, I(q)\, \mathrm{d}q \tag{4}$$

where $R(\langle q\rangle, q)$ is a resolution function describing the x-ray beam [22]. The $I(\langle q\rangle)$ function was fitted to the experimental data with a non-linear least squares procedure. The parameters of the fit are presented in table 2.

**Table 2.** Summary of the parameters used in the least squares fitting.

| | |
|---|---|
| $Sc_1$ | Global scale factor |
| $Sc_2$ | Microporosity scale factor |
| $C$ | Free parameter that ensures the Porod invariant equation |
| $A$ | Lattice parameter |
| $D$ | Domain size |
| $\nu$ | Peak shape parameter |
| $\sigma_a$ | Disorder parameter |
| $R_{in}$ | Pore radius |
| $\sigma_R/R$ | Relative polydispersity of radii |
| $R_{out}$ | Outer radius of the pores (including pore wall) |
| $r_{out}/r_{in}$ | Relative electronic density contrast |
| $R_g$ | Radius of gyration of micropores |
| $Sc_b$ | Constant background |
| $Sc_{extra}$ | Extra background scale factor |
| $q_g$ | Gaussian background position |
| $\sigma_g$ | Gaussian background peak width |

Fourier transform infrared spectrometry (FTIR) was performed at the Analytical Center of Chemistry Institute of the Sao Paulo University (USP) in a Bomem MB100 equipment to detect compositional changes in the material during the calcination process.

Scanning electron microscopy was performed in a field emission scanning electron microscope FEG100 JSM 7401F, operating at 1.0 kV in order to analyse the morphology of the calcined SBA-15 powder.

Nitrogen adsorption isotherm (NAI) measurements were executed at the Materials Science and Technology Center of Nuclear Energetic Research Institute—IPEN, using a Micromeritics ASAP 2010. The samples were degassed for 2 h at 100 °C, with the data acquisition being performed at 77 K, with relative pressure ranging from $10^{-6}$ to 0.995. Superficial areas were calculated with the Brunauer–Emmett–Teller (BET) equation [16, 17] and the pore size distribution was obtained with the Barrett–Joyner–Halenda (BJH) method [18].

The light scattering measurements to determine the particle size distribution of pristine and micronized SBA-15 powders were performed with Malvern Mastersizer S equipment at the Mines and Petroleum Department of the Polytechnic School—USP, using samples dissolved in alcohol. The micronization process was carried out in a conventional ball-milling machine from the pharmaceutical industry.

The proton induced x-ray emission (PIXE) experiments were performed at LAMFI[AQ: Please define 'LAMFI'], USP [19] in BALB/c calcined organs, which were treated orally or intramuscularly with silica powder. After a period of silica administration, the spleen, lungs, liver and kidneys of four mice were collected and calcined at 900 °C in order to detect the silicon atoms. For each experiment, a group of four mice were used as controls. In these experiments, a proton beam from the tandem accelerator hits the sample inducing ionization of the atoms. The decay of the electrons from upper levels to the lower ones is followed by x-ray emissions, which are detected in a Si(Li) solid-state detector. The emitted signals were fitted using standard software [20].

The experiments involving mice were approved by the Animal Ethical Committee of the Butantan Institute, Brazil, and followed protocols stated in the NIH Guide for Care and Use of Laboratory Animals.

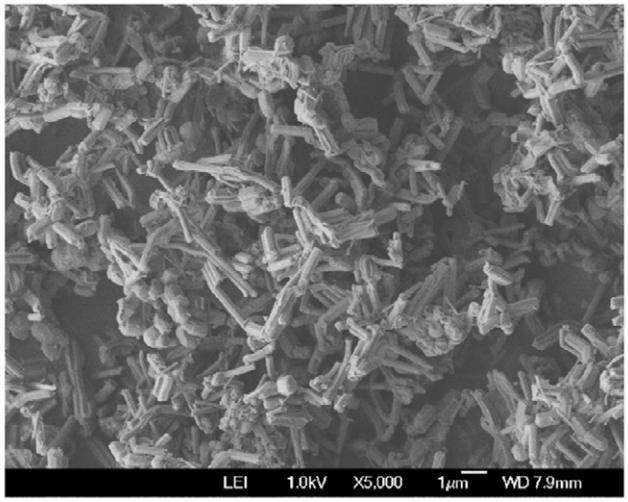


**Figure 1.** FEG Scanning electron microscopy of calcined SBA-15, showing silica cylinders of around 2 $\mu$m in length and macroporosity. The mesopores are inside the silica cylinders.

## 3. Results

### 3.1. Particle size distribution

Preliminary investigations demonstrated that the particle size of the silica powder is no larger than 35 $\mu$m. Attempts to reduce this value using an agate mortar were unsuccessful, as well as attempts of sifting the material through sieves of 20, 10 and 5 $\mu$m. Figure 1 depicts the morphology of the produced original material.

Due to the importance of particle size for the administration of SBA-15 as an adjuvant for vaccine delivery, the silica was processed in industrial pharmaceutical equipment. The resulting milled powder and the original material presented the particle size distribution showed in figure 2. The micronization process did not change any parameter by more than 15%, indicating an increased homogeneity in the particle size distribution. Also the diameter of larger particles was more affected than that of smaller particles, since the variation of $D(v, 0.9)$, a factor that represents the larger 10% of the particles, was larger than that of $D(v, 0.5)$, that represents either the larger or the smaller half of the particles. A SAXS analysis of pristine and micronized powders showed no difference in lattice parameter or integrated peak areas. Only a small intensity difference was observed at low $q$ ($q = (4\pi/\lambda)\sin q$) values due to the larger amount of empty spaces between micronized powder particles.

NAI measurements showed that the samples did not present any significant variation in the surface area, since the original SBA-15 sample possesses $S_{BET} = 624\,m^2\,g^{-1}$, while the micronized sample has $S_{BET} = 668\,m^2\,g^{-1}$. The pore volumes for the original and micronized samples are $0.9\,cm^3\,g^{-1}$ and $1.0\,cm^3\,g^{-1}$, respectively, with a mean pore size of 11.0 nm for both samples. Both SAXS and NAI results indicate that no significant changes in the material structure

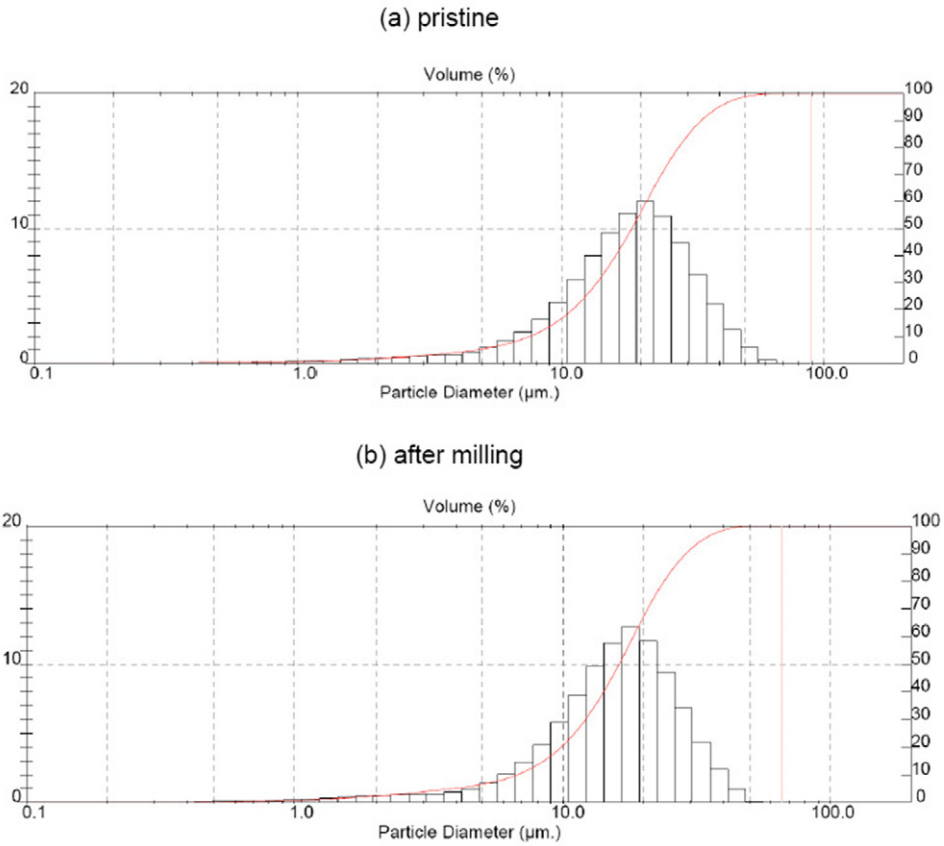


**Figure 2.** Particle size distribution of pristine and micronized SBA-15 powders. The mean particle size is around 20 $\mu$m for both samples.

occur during the micronization process, which is evidence of SBA-15's mechanical and structural stability. Visually comparing the original material with the micronized powder, the last one is thinner and more homogeneous, because in the processed material the particles are more sparsely distributed.

### *3.2. Incorporation of biological molecules*

The incorporation of BSA in SBA-15 silica was investigated: since BSA is a widely used experimental antigen it can, therefore, be characterized as a standard protein for this kind of incorporation study presented in this work. The objective is to investigate the use of a mesoporous silica material as an immune adjuvant, which in turn is responsible for enhancing the immune response [9, 10].

The SBA-15 plus BSA samples, named SF (stirring and filtering), SE (stirring and evaporation), RF (rest and filtering) and RE (rest and evaporation), were then characterized by SAXS and NAI.

Table 3 presents the total integrated peak area of the SAXS curves and $N_2$ adsorption results for SBA-15 mixed with BSA.

Figures 3(*a*) and (*b*) show the nitrogen isotherms and pore size distribution of the analysed samples, respectively. From the comparison between the RF and RE samples it is evident that the evaporation process is the best for incorporation, since all figures for adsorption results are lower for the sample that was dried through evaporation (table 3). All samples

**Table 3.** Total integrated peak area of the SAXS curves and $N_2$ adsorption results for SBA-15 mixed with BSA.

| Sample | SAXS peak area (a.u.) | $S_{BET}$ ($m^2\ g^{-1}$) | Pore volume ($cm^3\ g^{-1}$) | Pore size (nm) |
|---|---|---|---|---|
| SBA-15 | 10.6(2) | 668(7) | 1.0(1) | 11.0(1) |
| SE | 2.7(2) | 135(1) | 0.3(1) | 10.6(1) |
| SF | 6.6(2) | 148(1) | 0.3(1) | 10.6(1) |
| RE | 2.7(2) | 72(1) | 0.2(1) | 10.0(1) |
| RF | 6.7(2) | 186(2) | 0.4(1) | 11.0(1) |

presented similar SAXS results for the lattice parameter, around 12.5(3) nm. Integrated peak areas, however, varied greatly, as shown in table 3. These intensities were smaller for the samples dried through evaporation. Also, when comparing mixture methods, the results were similar, but the evaporated samples presented a lower peak area indicating a higher degree of BSA plus PBS loading into the mesoporous structure. These results are consistent with those obtained from NAI, showing that the sample which was kept at rest and evaporated (RE), when compared to the filtered (RF) one, possessed a lower specific surface area and pore volume, which were also significantly less when compared to its stirred counterpart. The combination of results for mixture methods and drying methods indicate that the best approach for the incorporation of biologically remarkable molecules consists in keeping the solution at rest and drying it through evaporation (RE), and therefore all of the following results were obtained from samples prepared through this method.

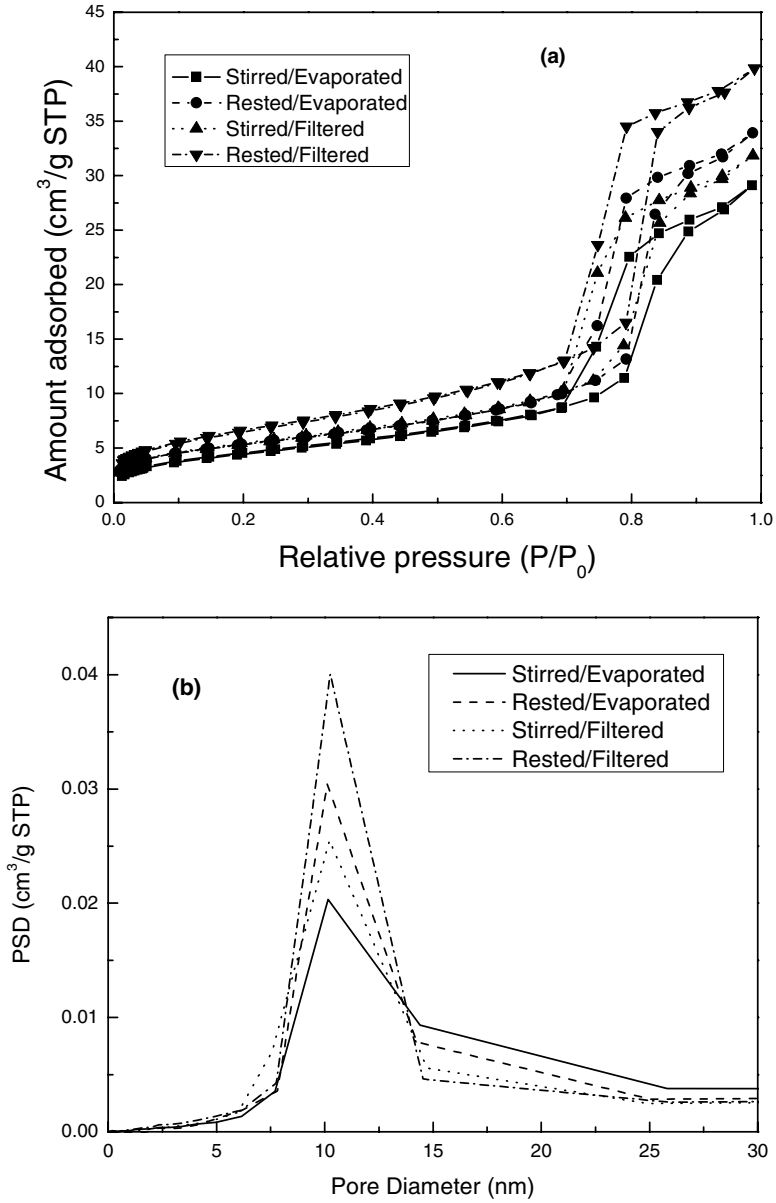


**Figure 3.** (*a*) Nitrogen sorption isotherm (NSI) (*b*) and pore size distribution of all incorporation methods. The NSI and $S_{BET}$ and pore volume (table 3) point to RE as the best route for incorporation into the pore structure. The open mesopores have identical diameters of ∼10 nm.

Figure 4 presents the SAXS results of BSA release in PBS. There is a systematic evolution of the scattered intensity, showing an overall decrease of the scattered intensity with time, related to a change in relative electronic density contrast; this evolution of the scattering curve represents the release of BSA from the silica matrix, while PBS fills the open spaces left behind by BSA molecules. In figure 5(*a*) the SAXS curves obtained during the release of BSA in the gastric fluid present a dynamic behaviour: the first two frames (6 and 12 h) are very similar, followed by a slightly higher curve for the frame obtained at 18 h (especially between 0.02 and 0.05 $Å^{-1}$). After that, all other frames (24–48 h) are, again, similar, with a few differences in the interference peaks related to the porous structure. This suggests a transition occurring between 12 and 24 h, related to the release of BSA from the SBA-15 matrix. A non-linear least squares fit with the presented model reveals an increase in the scale factor related to the larger objects, which is accompanied by a decay in the global scale factor. This suggests the release of BSA and its aggregation outside the pores. Figure 5(*b*) presents the SAXS curves of BSA release from SBA-15, but with Eudragit. There is an analogous transition, albeit shifted to a higher time frame (the 36 h frame, between 30 and 42 h). Similarly to what happens in the sample without Eudragit, the scale factor accounting for larger objects suffers a dramatic increase simultaneously with the global scale factor, revealing a delay in the release and aggregation of BSA. This behaviour is compatible with findings that the polymer acts as a protection from BSA lixiviation, retarding the release of BSA from SBA-15 in the gastric fluid. Figures 6(*a*) and (*b*) show the SAXS curves of BSA release in the intestinal fluids, without and with Eudragit, respectively. In figure 6(*a*) there is only a slight difference in the intensity of the curve obtained

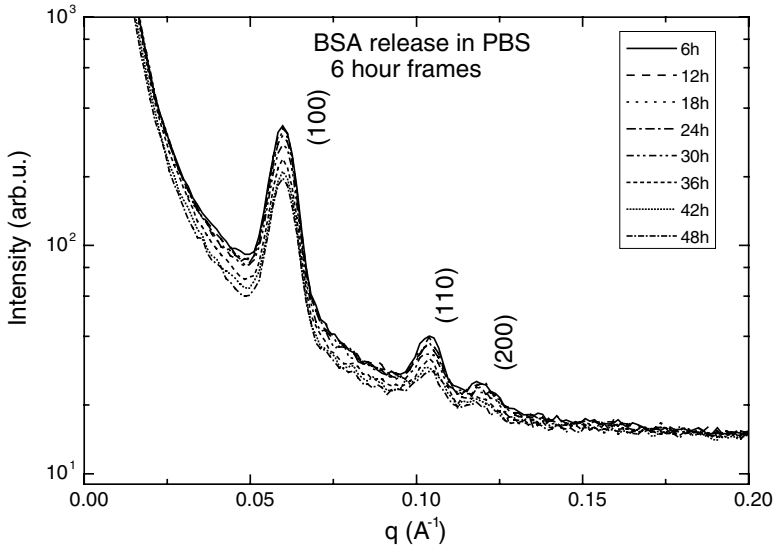


**Figure 4.** SAXS curves obtained *in situ* during experiments of BSA release from SBA-15 after incorporation through the RE route in PBS.

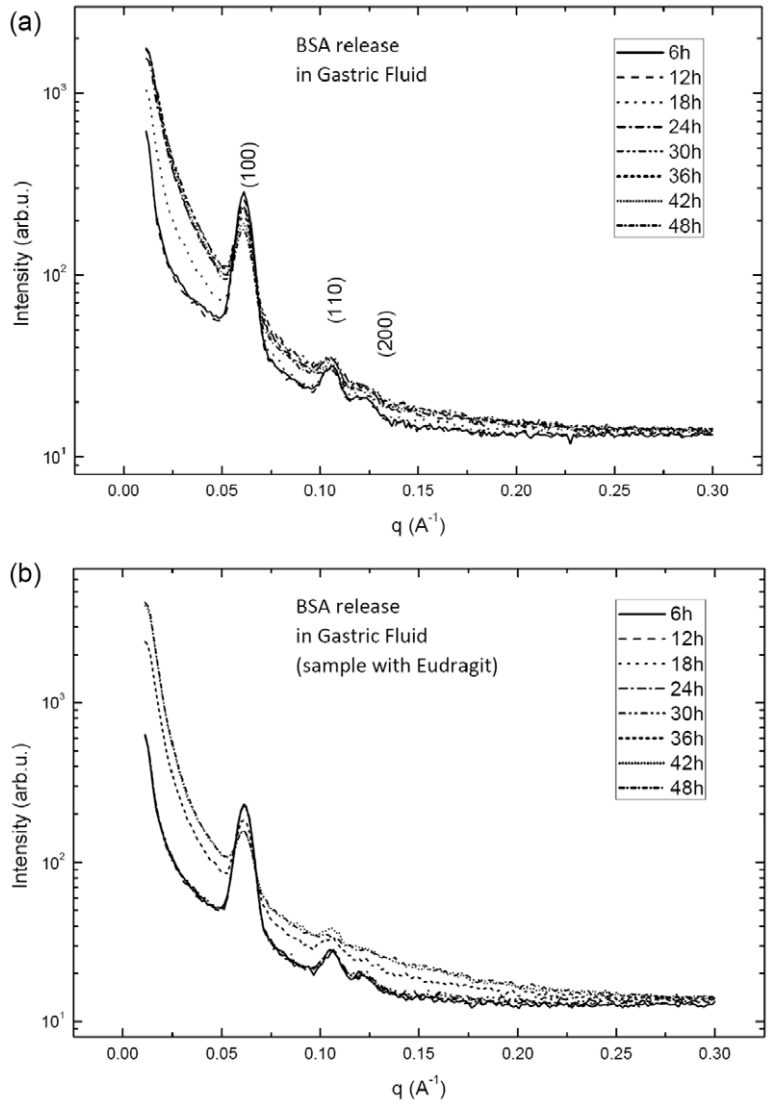


**Figure 5.** SAXS curves obtained *in situ* during experiments of BSA release from SBA-15 after incorporation through the RE route in (*a*) gastric fluid and (*b*) plus Eudragit in gastric fluid.

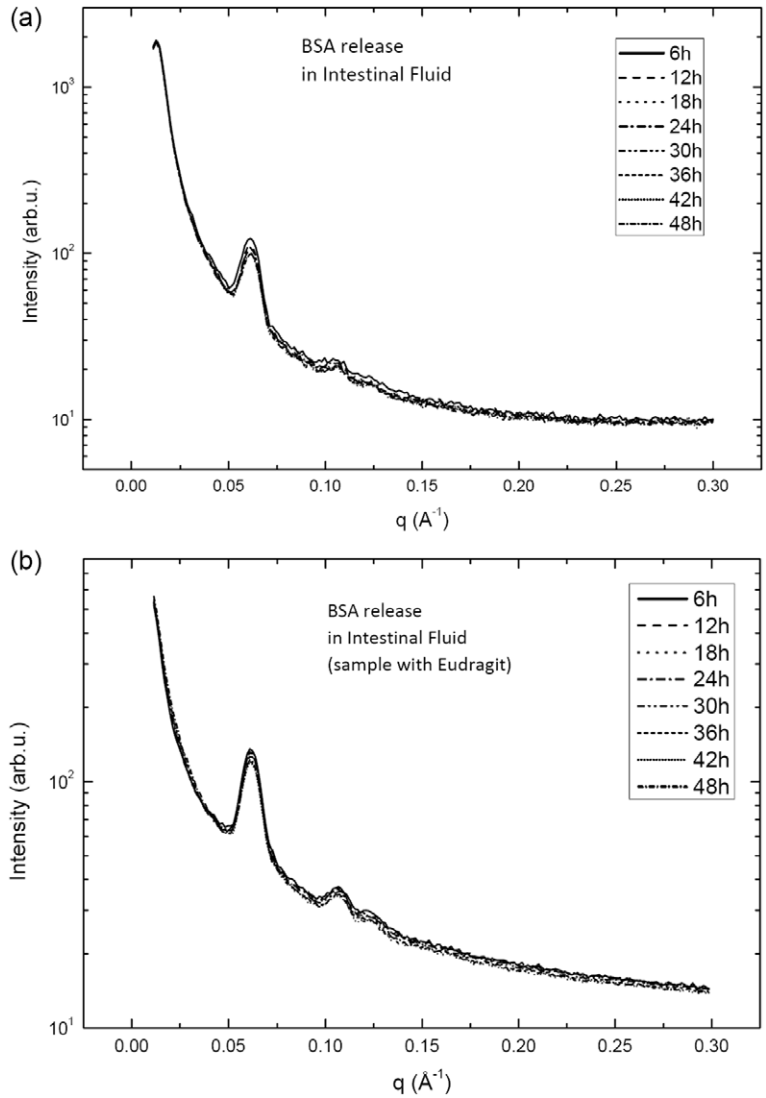


**Figure 6.** SAXS curves obtained *in situ* during experiments of BSA release from SBA-15 after incorporation through the RE route in (*a*) intestinal fluid and (*b*) plus Eudragit in intestinal fluid.

at 6 h compared to all other data. This is an indication that the release happened before 6 h. In the presence of Eudragit there is no remarkable difference to the curves obtained from the samples without the polymer, a finding that is consistent with the pH-sensibility of Eudragit.

For the *ex situ* experiments, with dried SBA-15 plus BSA, it is possible to calculate, from the SAXS experiments and data fitting, the variation in the electronic density due to the presence of BSA inside the pores. On the other hand for the *in situ* experiments in complex media, due to the low electronic contrast between the silica walls and BSA, both composed of light elements, this calculation cannot be performed. The *in situ* SAXS results and model do not present enough resolution to distinguish variations in the electronic density inside the pores. Therefore, our conclusions were based on variations in the whole scattered intensities, by analysing scale factors.

The study of silicon in mice organs by PIXE was performed in experimental groups as shown in table 4. Figures 7(*a*)–(*c*) presents the silicon content in all analysed mice organs and control samples. In these figures, the limits correspond to the silicon content in the control, which in our experiment was 354 ppm, since this element is present in food in the form of silica. In these figures the corresponding limit is dashed with error bars in all points. No silicon content was detected above the control in the liver. The results showed that the deposition of silicon is eliminated in all organs in few days, but it remains in the spleen after 35 days, being completely eliminated from the organism after 70 days.

**Table 4.** Experimental Balb-C mice groups used in the PIXE detection of Si.

| Administration time | Control | Oral via | Intramuscular via |
|---|---|---|---|
| 6 hours | | vo6 | |
| 1 day | c1 | vo1 | im1 |
| 35 days | c35 | vo35 | im35 |
| 70 days | | vo70 | |

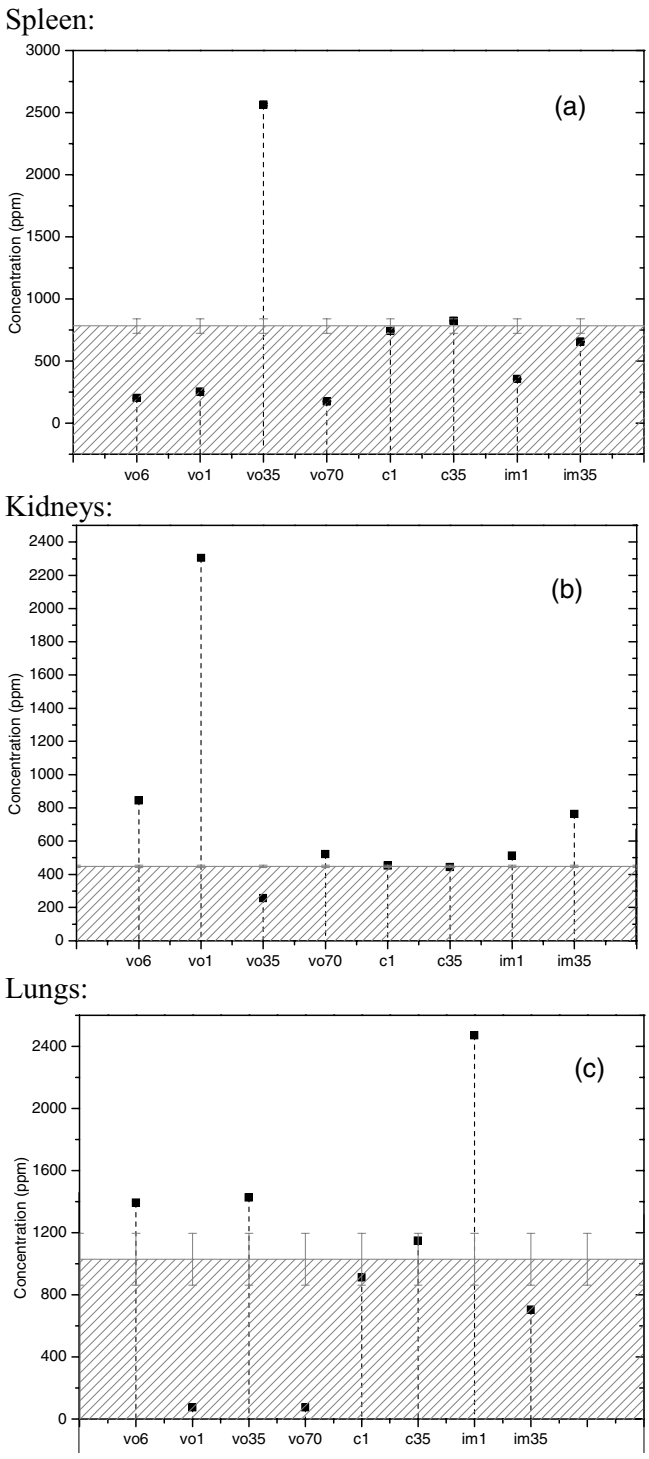


**Figure 7.** PIXE results of silicon concentration in (*a*) spleen, (*b*) kidneys and (*c*) lungs for oral (vo) and intramuscular (im) administration on a function of time: 1 day, 7, 35 and 70 days.

### *3.3. Immunological tests*

The adjuvant effect and toxicity of the ordered mesoporous SBA-15 silica sample were evaluated through a comparative study using the conventional adjuvant $Al(OH)_3$. BSA was given to genetically selected $L_{III}$ and $L_{IVA}$ low responder and the $H_{III}$ and $H_{IVA}$ high responder mouse lines in $Al(OH)_3$ or SBA-15 [9, 10]. The results proved that SBA-15 increased

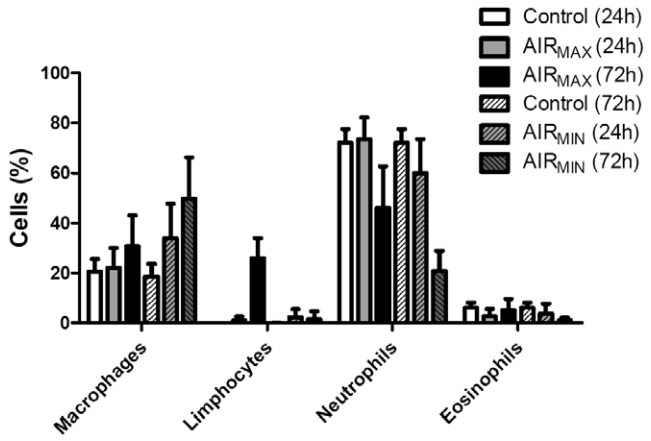


**Figure 8.** Inflammatory response against SBA-15 in the control, high responder ($AIR_{max}$) and low responder ($AIR_{min}$) mice, measured 24 and 72 h after administration.

the IgG anti-BSA production when compared to $Al(OH)_3$, especially in low responder mice.

The inflammatory response was evaluated by a study in which the effect of SBA-15 was analysed *in vivo* in the genetically selected mice lines for maximal ($AIR_{max}$) and minimal ($AIR_{min}$) acute inflammatory reactivity. Through the air pouch model of inflammation, distinct concentrations (from 250 to 2500 $\mu g\,ml^{-1}$) of SBA-15 in PBS were given subcutaneously; the control group received PBS and was also monitored. The contents (cells and proteins) of the air pouch were removed after different periods (24–96 h) to analyse the inflammatory response. After 24 h it was observed that neutrophils were predominant and after 72 h, macrophages were predominant in both mouse lines as shown in figure 8; it is important to point out that these antigen presenting cells (APCs) are essential for building an effective immune response.

## 4. Discussion

The proper and reproducible production of ordered mesoporous SBA-15 silica is an important issue when dealing with its use for biological purposes. In this paper, we demonstrated that the chosen preparation procedure is reproducible concerning the structural and morphological characteristics of the powder samples. It has already been proven that SBA-15 is a promising immunological adjuvant [9, 10, 14], but it is important to know how this silica interact with organs and how it is eliminated, as well as other mechanisms of action of the particles as a vehicle to antigen presentation. In particular, tests with BSA indicated that SBA-15 forms a barricade to prevent the protein degradation in the stomach and digestive tract, as well as inducing immunity heavily dependent on the architecture of the porous silica. The BSA deliverance is pH sensitive [24], being released at a higher pH when encapsulated in polyacrylic acid plus SBA-15. This combination of adjuvants, similar to our results with Eudragit, protected the antigen in the stomach (pH 1–3) and allowed for the release to the intestine (pH 6–8), the natural residence and the rich supply of immune competent cells. Considering the isoelectric point

of BSA at a pH equal to 4.8, it is reported that the release of BSA increases the pH to 6–7 [23].

The protection of SBA-15 is not limited to the pH, but also to protease action and thermal variations, an important issue for vaccination purposes [25]. Also, our results demonstrate the stability of SBA-15 under physiological conditions. Previous results also showed that after 10 days in NaCl, SBA-15 degradation is low and only after 60 days is there the loss of ordered mesoporous arrangement [26]. Concerning the vaccination purposes of SBA-15, the low lixiviation proves that it is a strong adjuvant candidate. Also, the safety of SBA-15 is an important issue for vaccination and drug delivery purposes. Our results show that it does not affect cell integrity [10], and other researchers revealed that even in the blood circulation no abnormal behaviour or symptoms were observed in treated mice [27].

The incorporation of biomolecules in SBA-15 depends on the pore size. The samples produced in this work possess a mean pore diameter of around 10 nm, a size that allows BSA to be entrapped inside the pores or to cover the pore opening in a cork-like manner. The incorporation capacity depends on the material's architecture, adsorption method, interaction between the surface of mesoporous material and proteins, besides time and pH [28]. SBA-15 has the potential for a broad range of applications as an adsorbent [29]. Recent work reports the use of SBA-15 as a carrier for poorly soluble drugs for oral administration. In this case, as found in this work, an efficient drug loading was achieved by evaporation, allowing a rapid matrix inhibition [30].

The PIXE analysis of the organs had the objective to determine the amount of silicon from the SBA-15 agglomerated in the organs, mostly concerning its elimination after a certain period of time. All the results are based on comparison of the silicon content in the control mice (dashed area), because silicon is present in mice food. Figure 7 shows results for oral (vo) and intramuscular (im) administrations. In the spleen, silicon was detected after 35 days in oral administration, which is an important finding since active immunity is generated in this organ. In kidney and lungs it was observed that the amount of silicon is larger than the control for the first periods of administration (6 hours and 1 day). Since vaccination is a non-daily treatment, the fact that silicon is totally eliminated from all organs after 70 days gives an excellent indication of the use of SBA-15 as an immunological adjuvant, as it is important to guarantee the natural removal of the adjuvant from all organs. All the results showed an excellent indication of the use of SBA-15 as an immunological adjuvant, mainly in both APCs, i.e., macrophages and neutrophils. It must be stressed that, especially in the $AIR_{MIN}$ mice, these activations are significant even in these constitutively very-low inflammatory reactive individuals. Thus, the antigen maintained in these APCs determines the high potential of immune acquired responsiveness induced by the SBA-15 administration. Another relevant fact is that there is no activation of eosinophils, cells responsible for allergic responses. As expected, the stimulation of lymphocytes, the main protagonists of the acquired immune response, will be relevant only after at least 96 h of immunization. Even though other studies reported a degree of toxicity of mesoporous silicates [31], our researches, including the present one and others, did not find any deleterious behaviour of SBA-15 on mice cells [9, 10, 32].

## 5. Conclusions

Here, a reproducible method to prepare the nanostructured silica SBA-15, providing a porous matrix with a mean pore diameter of 10 nm into which molecule can be incorporated was described.

SBA-15 and BSA released under body fluid conditions revealed that this silica and, more importantly, the encapsulated protein, is still very stable in acidic and basic media.

The localization of silicon in mice organs indicated that there is no residue in the liver/lungs. For the other organs, silicon was found in the spleen after 35 days, being completely eliminated after 10 weeks. Immunological studies showed that SBA-15 presents a high strength adjuvant characteristic when compared to the traditional $Al(OH)_3$ [10], and does not present toxicity, improving the immunological response by inducing an inflammatory response as well as increasing the phagocyte activity by APCs such as macrophages and dendritic cells.

## Acknowledgments

Thanks are due to Professor I C Consentino for the use of $N_2$ adsorption equipment. The financial support from Cristália Produtos Farmacêuticos Ltda., FAPESP, CNPq, INCTTOX and CeTICS Programs are acknowledged.

## References

[1] Kresge C T, Leonowicz M E, Roth W J, Vartuli J C and Beck J S 1992 Ordered mesoporous molecular-sieves synthesized by a liquid-crystal template mechanism *Nature* **359** 710–12

[2] Zhao D Y, Feng J L, Huo Q S, Melosh N, Fredrickson G H, Chmelka B F and Stucky G D 1998 Triblock copolymer syntheses of mesoporous silica with periodic 50 to 300 angstrom pores *Science* **279** 548–2

[3] Jaroniec M 2006 *Combined and Hybrid Adsorbents: Fundamentals and Applications* (Springer: Berlin) pp 23–6

[4] Somorjai G A, Tao F and Park J Y 2008 The nanoscience revolution: merging of colloid science, catalysis and nanoelectronics *Top. Catal.* **47** 1–14

[5] Charnay C, Begu S, Tourne-Peteilh C, Nicole L, Lerner D A and Devoisselle J M 2004 Inclusion of ibuprofen in mesoporous templated silica: drug loading and release property *Eur. J. Pharmaceutics Biopharmaceutics* **57** 533–40

[6] Lu J, Liong M, Zink J I and Tamanoi F 2007 Mesoporous silica nanoparticles as a delivery system for hydrophobic anticancer drugs *Small* **3** 1341–6

[7] Slowing II, Trewyn B G, Giri S and Lin V S Y 2007 Mesoporous silica nanoparticles for drug delivery and biosensing applications *Adv. Funct. Mater.* **17** 1225–36

[8] Fagundes L B, Sousa T G F, Sousa A, Silva V V and Sousa E M B 2006 SBA-15-collagen hybrid material for drug delivery applications *J. Non-Cryst. Solids* **352** 3496–501

[9] Mercuri L P *et al* 2006 Ordered mesoporous silica SBA-15: a new effective adjuvant to induce antibody response *Small* **2** 254–6
[10] Carvalho L V, Ruiz R C, Scaramuzzi K, Marengo E B, Matos J R, Tambougi D V, Fantini M C A and Sant'Anna O A 2010 Immunological parameters related to the adjuvant effect of the ordered mesoporous silica SBA-15 *Vaccine* **28** 7829–36
[11] Ambrogi V, Perioli L, Pagano C, Marmottini F, Ricci M, Sagnella A and Rossi C 2012 Use of SBA-15 for furosemide oral delivery enhancement *Eur. J. Pharm. Sci.* **46** 43–8
[12] Wang T, Jiang H, Zhao Q, Wang S, Zou M and Cheng G 2012 Enhanced mucosal and systemic immune response obtained by porous silica nanoparticles used as an oral vaccine-adjuvant: effect of silica architecture on immunologial properties *Int. J. Pharmac.* **436** 351–8
[13] Mody K T, Popat A, Mahony D, Cavallaro A S, Yu C and Mitter N 2013 Mesoporous silica nanoparticles as antigen carriers and adjuvants for vaccine delivery *Nanoscale* **5** 5167–79
[14] 2007 *International Patent* WO 07030901
[15] Matos J R, Mercuri L P, Kruk M and Jaroniec M 2001 Toward the synthesis of extra-large-pore MCM-41 analogues *Chem. Mater.* **13** 1726–31
[16] Kruk M, Jaroniec M and Sayari A 1999 Relations between pore structure parameters and their implications for characterization of MCM-41 using gas adsorption and x-ray diffraction *Chem. Mater.* **11** 492–500
[17] Brunauer S, Emmett P H and Teller E 1938 *J. Am. Chem. Soc.* **60** 309–19
[18] Barrett E P, Joyner L G and Halenda P P 1951 The determination and area distributions in porous substances: part 1. Computations from nitrogen isotherms *J. Am. Chem. Soc.* **73** 373–80
[19] www2.if.usp.br/∼lamfi/
[20] 2006 IAEA LaboratoriesWinQXAS *www.iaea.org/OurWork/ST/NA/NAAL/pci/ins/xrf/pci.XRFdown.php*
[21] Sundblom A, Oliveira C L P, Palmqvist A E C and Pedersen J S 2009 Modeling *in situ* small-angle x-ray scattering measurements following the formation of mesostructured silica *J. Phys. Chem.* C **113** 7706–13
[22] Pedersen J S, Posselt D and Mortensen K 1990 Analytical treatment of the resolution function for small angle scattering *J. Appl. Crystallogr.* **23** 321–33
[23] Nguyen T P B, Lee J W, Shim W G and Moon H 2008 Synthesis of functionalized SBA-15 with ordered large pore size and its adsorption properties of BSA *Microporous Mesoporous Mater.* **110** 560–9
[24] Song S W, Hidajat K and Kawi S 2007 pH-controllable drug release using hydrogel encapsulated mesoporous silica *Chem. Commun.* 4396–8
[25] Makidon P E *et al* 2008 Pre-clinical evaluation of a novel nanoemulsion-based hepatitis B mucosal vaccine *Plos One* **8** e2954
[26] Izquierdo-Barba I, Colilla M, Manzano M and Vallet-Regí M 2010 *In vitro* stability of SBA-15 under physiological conditions *Microporous Mesoporous Mater.* **132** 442–52
[27] He Q, Zhang Z, Gao F, Li Y and Shi J 2010 *In vivo* biodistribution and urinary excretion of mesoporous silica nanoparticles: effects of particle size and PEGylation *Small* **7** 271–80
[28] Liu X, Zhu L, Zhao T, Lan J, Yan W and Zhang H 2011 Synthesis and characterization of sulfonic acid-functionalized SBA-15 for adsorption of biomolecules *Microporous Mesoporous Mater.* **142** 614–20
[29] Wu Z and Zhao D 2011 Ordered mesoporous materials as adsorbents *Chem. Commun.* **47** 3332–8
[30] Ambrogi, V, Perioli L, Pagano C, Marmottini F, Ricci M, Sagnella A and Rossi C Use of SBA-15 for furosemide oral delivery enhancement *Eur. J. Pharm. Sci.* **46** 43–8
[31] Hudson S P, Padera R F, Langer R and Kohane D S 2008 The biocompatibility of mesoporous silicates *Biomaterials* **29** 4045–55
[32] Radin S, Falaize S, Lee M H and Ducheyne P 2002 *In vitro* bioactivity and degradation behavior of silica xerogels intended as controlled release materials *Biomaterials* **23** 3113–22